KAPL-P-000179
(K97069)
CONF-971005--

A MONTE-CARLO METHOD FOR EX-CORE NEUTRON RESPONSE

R. G. Gamino, J. T. Ward, et. al.

October 1997

KAPL ATOMIC POWER LABORATORY SCHENECTADY, NEW YORK 10701

Operated for the U. S. Department of Energy
by KAPL, Inc. a Lockheed Martin company

DISCLAIMER

DISCLAIMER

Portions of this document may be illegible in electronic image products. Images are produced from the best available original document.

A MONTE CARLO METHOD FOR EX-CORE NEUTRON RESPONSE

Ray G. Gamino, John T. Ward, and Jeffrey C. Hughes

Lockheed Martin Corporation
P.O. Box 1072
Schenectady, NY 12301-1072
Tel: 518-395-4942; Fax: 518-395-4422

ABSTRACT

A Monte Carlo neutron transport kernel capability primarily for ex-core neutron response is described. The capability consists of the generation of a set of response kernels, which represent the neutron transport from the core to a specific ex-core volume. This is accomplished by tagging individual neutron histories from their initial source sites and tracking them throughout the problem geometry, tallying those that interact in the geometric regions of interest. These transport kernels can subsequently be combined with any number of core power distributions to determine detector response for a variety of reactor conditions. Thus, the transport kernels are analogous to an integrated adjoint response. Examples of pressure vessel response and ex-core neutron detector response are provided to illustrate the method.

INTRODUCTION

This paper describes a Monte Carlo transport kernel capability, which has been incorporated into the RACER continuous energy Monte Carlo code[1]. The method was briefly introduced in Reference 2. This paper further describes the method and presents results to illustrate uses of the method. The transport kernels represent a Green's function for neutron transport from a fixed source volume out to a particular volume of interest. Also, since kernels are evaluated numerically by Monte Carlo, the problem geometry can be arbitrarily complex, yet exact.

This method is intended for problems where an ex-core neutron response must be determined for a variety of reactor conditions. Two examples are ex-core neutron detector response and pressure vessel fluence. The kernels may also be used in conjunction with power distributions from a spatial kinetics code or a core-follow model to determine time-dependent detector responses. In this manner, the transport kernels may be used with various on-line core monitoring systems.

The total response is expressed in terms of neutron transport kernels weighted by a core fission source distribution. In these types of calculations, the response must typically be computed for hundreds of source distributions, but the transport kernels only need to be calculated once. In this way, the transport kernels are analogous to an integrated adjoint response and are used just like adjoint responses. The advance described in this paper is that the kernels are generated with a highly accurate 3-D Monte Carlo transport calculation, instead of an approximate method such as a synthesized 3-D discrete ordinates solution.

METHOD DESCRIPTION

The Monte Carlo detector response kernels are isotopic reaction rate or flux edits which represent source-to-capture transport kernels. Formally, these kernels represent a specific reaction rate with the nuclide of interest, or the scalar flux, in a detector volume due to the fraction of source neutrons originating in the core from a particular source volume. Both the source volumes and detector volumes are defined within the Monte Carlo problem geometry. The reference to a "detector" is used loosely since any volume, or set of volumes, in the problem can be defined as the detector.

The directional flux density, Ψ, at a point in phase space, $(\underline{r}, \underline{\Omega}, E)$, caused by a distributed source may be given by the Green's function superposition integral[3]

$$\Psi(\underline{r}, \underline{\Omega}, E) = \int dV_0 \int d\underline{\Omega}_0 \int dE_0 \; G(\underline{r}_0, \underline{\Omega}_0, E_0 \rightarrow \underline{r}, \underline{\Omega}, E) \; Q(\underline{r}_0, \underline{\Omega}_0, E_0) \qquad \text{Eq. (1)}$$

where the Green's function, $G(\underline{r}_0, \underline{\Omega}_0, E_0 \rightarrow \underline{r}, \underline{\Omega}, E)$, represents the directional flux density at $(\underline{r}, \underline{\Omega}, E)$ due to a unit point source located at $(\underline{r}_0, \underline{\Omega}_0, E_0)$ with Q the source density distribution. Equation (1) can be generalized from a point in phase space to an integral over a portion of phase space, for example a detector volume designated V_d. This enables Monte Carlo to be used effectively by tracking neutrons from the source volume, V_0, and scoring them if they undergo an interaction in the volume of interest, V_d. Monte Carlo is particularly well suited to general cases where the geometry is non-uniform or complex and the Green's functions are not given by any simple analytic expressions.

Equation (1) can also be generalized to a reaction rate density at point $(\underline{r}, \underline{\Omega}, E)$, and then integrated over the volume of interest, to determine the total number of type-α reactions per second in the detector volume, V_d. Further, if the total source volume, V_0, is divided into N source volumes, V_n, Equation (1) can then be generalized to

$$\int dV_d \int d\underline{\Omega} \int dE \; \Sigma_\alpha(\underline{r}, E) \; \Psi(\underline{r}, \underline{\Omega}, E) = \sum_{n=1}^{N} Q_n \; K(n \rightarrow d) \qquad \text{Eq. (2)}$$

where

$$Q_n = \int dV_n \int d\underline{\Omega}_0 \int dE_0 \; Q(\underline{r}_0, \underline{\Omega}_0, E_0) \qquad \text{Eq. (3)}$$

= total number of source neutrons in volume V_n, and

$$K(n \rightarrow d) =$$

$$\frac{1}{Q_n} \int dV_n \int d\underline{\Omega}_0 \int dE_0 \; Q(\underline{r}_0, \underline{\Omega}_0, E_0) \int dV_d \int d\underline{\Omega} \int dE \; \Sigma_\alpha(\underline{r}, E) \; G(\underline{r}_0, \underline{\Omega}_0, E_0 \rightarrow \underline{r}, \underline{\Omega}, E) \qquad \text{Eq. (4)}$$

= the transport kernel, i.e., number of type-α reactions per second in detector volume, V_d, per source neutron in volume V_n.

RACER produces reaction rate edits which are automatically normalized to a total integrated source of one neutron. If a unit source density is specified for each source node for transport kernel generation, the total source in each node V_n will be V_n/V_0 source neutrons. The Monte Carlo tallied results (transport kernels) are then $K^{MC}(n \rightarrow d) \equiv$ Monte Carlo transport kernel; type-α reaction rate in detector volume V_d due to V_n/V_0 source neutrons in volume V_n for each source/detector volume pair, (V_n, V_d). These are smaller than the kernels in Equation (4) by the factor V_n/V_0.

The proper weighting functions to use with the Monte Carlo kernels are relative power densities, $S_{n,c}$ (in volume V_n for core condition c), which are given by

$$S_{n,c} \equiv \frac{P_{n,c}/V_n}{P_0/V_0} \qquad \text{Eq. (5)}$$

where $P_{n,c}$ is the total power in volume V_n, and P_0 is the total power in the core. The relative power densities must be on a consistent basis with the kernel source volumes in the Monte Carlo analysis, and should also be normalized such that the corresponding power fractions sum to one. The total reaction rate (type-α reactions per second per source neutron) in detector volume V_d, for core condition c, is obtained by multiplying the Monte Carlo kernels by $S_{n,c}$ and summing over all source regions, and is given by

$$\int dV_d \int d\underline{\Omega} \int dE \Sigma_\alpha(\underline{r}, E) \Psi(\underline{r}, \underline{\Omega}, E) = \sum_{n=1}^{N} S_{n,c} K^{MC}(n \rightarrow d) \equiv \sum_{n=1}^{N} \frac{P_{n,c}}{P_0} K(n \rightarrow d) \qquad \text{Eq. (6)}$$

Equation (6) can be generalized to multiple detector volumes and group-wise kernels in a straightforward manner. The user may decide to model a specific "detector" as a series of sub-volumes. Also, RACER generates group-wise transport kernels $K_g^{MC}(n \rightarrow d)$ which represent the number of type-α reactions per second in detector volume V_d and energy range ΔE_g per V_n/V_0 source neutrons in source volume V_n. The total detector response (reaction rate) per source neutron, for core condition c, integrated over energy, all source volumes, and all detector volumes is then given by

$$R_c = \sum_{d=1}^{D} \sum_{n=1}^{N} S_{n,c} \sum_{g=1}^{G} K_g^{MC}(n \rightarrow d) \qquad \text{Eq. (7)}$$

where D is the total number of detector volumes, N is the total number of source volumes, and G is the total number of energy groups in the Monte Carlo tallies or edits.

The real power of this method is utilized by generating the transport kernels for a spatially flat source distribution (unit source density within each source volume V_n) within the core. Once a set of detector response kernels has been generated, it can be combined with a particular power distribution to obtain the integrated detector response as shown in Equations (6) and (7). Combining the transport kernels and particular core power distributions is efficient, and may be performed as many times as required to obtain a set of integrated responses. The use of Monte Carlo methods to generate the kernels is very attractive because with current editing capabilities all of the kernels can be generated concurrently in one computer run.

The specific nuclide and the reaction of interest must be specified. User specified options include absorption rate for a single nuclide, or absorption rate, nu-fission rate, or flux-volume for the entire detector volume composition. The user may request all of these options simultaneously.

Method Approximations

The transport kernels are time-independent. This means that no allowance is made for material burnup, control rod motion, etc. For typical applications, e.g., vessel fluence or ex-core detector response, only high energy or fast neutrons originating in the core ultimately interact with the detector volume of interest. Since fast neutron attenuation is about the same through various core materials, the assumption of time-independent kernels is valid. This assumption has been supported numerically through sensitivity studies.

The kernels are generated using a uniform source distribution within each source region. For ex-core detector response or pressure vessel fluence calculations, the source regions near the core periphery are the most important. Sufficiently small source regions in this area of high importance should be used to retain high accuracy.

Advantages

- Highly accurate continuous energy Monte Carlo neutron transport physics is used.
- Model geometry can be arbitrarily complex. Very detailed regions can be modeled with high precision.
- Transport kernels are generated concurrently in one run, for any number of source and detector regions, as well as for any number of reaction types.
- The detector transport kernels can be edited over any user-specified energy range.
- The methodology to evaluate detector responses is very efficient, since the kernels can be combined with any number of source distributions. The kernels are essentially an integrated adjoint detector response.

Other Considerations

- Since an explicit 3-D transport analysis of the model geometry is performed, the resulting kernels will only be valid for a particular physical arrangement. Kernels must be regenerated to

accommodate any change in ex-core geometry, for example the positioning of shielding materials.
• Running time can be significant as there may be several orders of magnitude attenuation between the core and the detectors. It should be noted that the kernel tallies themselves do not consume any significant additional CPU time over and above the neutron tracking.
• Individual kernels can have large statistical uncertainties.
• A spatially flat fixed source density is assumed within each source volume. Note that the energy distribution of the starting neutrons follows a fission spectrum.

APPLICATION AND RESULTS

Importance Sampling - Splitting/Rouletting Weights

It is important that variance reduction techniques such as splitting and rouletting be employed in detector response calculations. These are required to obtain statistically meaningful answers in a reasonable amount of computer time. Splitting and rouletting based on energy- and region-dependent importance weights are the methods used in RACER. The goal is to enhance the population of desirable neutrons only, in the directions of the detector volume, as well as energies of most interest. Each importance region is assigned a set of weights. These weights are used such that the total weight of the split or rouletted particles is conserved (i.e., equal to the original single particle) so that no statistical bias is introduced.

Splitting weights will decrease as distance from the core increases to enhance the number of neutrons. The goal is to have a relatively constant particle population at high energies, from the core to the detectors. Both spatial and energy distributions of the neutron flux must be considered in determining weights.

An adjoint function is extremely useful for weight determination. An adjoint function may be obtained from a discrete ordinates code. Even an adjoint for a simplified 1-D or 2-D representation of the problem geometry typically provides very useful information. Alternatively, specific code-dependent edits such as the number of flights and collisions in each volume or surface edits for boundary crossings are available, and can be used to provide feedback on the particle population. A few iterations using these edits can significantly improve the weights.

Pressure Vessel Fluence Results

For the purposes of illustrating the method, a geometry of a typical commercial pressurized water reactor (PWR) has been used. This problem (Model Problem 1) is not meant to represent any specific reactor, but to have dimensions and compositions which are representative of a large commercial power reactor. The radial geometry is shown in Figure 1. A 1/8 core model has been used, due to azimuthal symmetry. The axial geometry is shown in Figure 2. Due to axial symmetry, a 1/2 core model has been used.

The core source regions are defined as assembly-sized regions, divided into ~4.5 inch regions axially for a total of 510 (34x15) source regions. The pressure vessel itself is broken up radially (~1.5 inch regions), azimuthally (3 degree regions), and axially (~3.5 inch regions) into a total of 2,700 regions. This results in 1.377×10^6 (510x2,700) transport kernels. For this case, the transport kernels have been defined as the flux in each particular pressure vessel sub-volume, rather than a reaction rate. Two energy ranges of interest were investigated: >1MeV and 100keV - 1MeV. The source within the core was spatially flat with a unity fission density in each source volume.

Figures 3-6 provide results from the RACER calculations. Note that radial node 1 is nearest the core, axial node 1 is directly above the core mid-plane, and azimuthal node 1 is along the x-axis in Figure 1. Slightly more than 1 billion neutron histories were computed, which, when combined with judicious splitting / rouletting windows, resulted in 2σ or 95% confidence interval uncertainties for pressure vessel regions opposite the active core height of 1-2%, and ~10% 2σ uncertainties for the uppermost nodes in the model.

Figure 4 shows a large decrease in neutron flux from the axial region adjacent to the core to the higher elevations. These results are expected as the path length from the core to these regions increases. Figures 3 and 4 show approximately a factor of ten reduction in the > 1 MeV flux from the radial interior to the exterior of the vessel, caused by the slowing down of neutrons from interactions with iron. Figure 3 also displays a strong azimuthal dependence based on varying reflector thickness.

Figure 5 displays four individual response kernels versus axial height in the core for two source regions to two specific pressure vessel regions. Note that for the values below $\sim 10^{-12}$, the statistical uncertainties are quite large, but these kernels provide very little overall response. Note that additional detail within core periphery regions may be desirable to provide a more accurate source description for the majority of the neutrons which contribute to the flux in the pressure vessel.

Figure 6 shows the ratio of flux for neutrons between 100 keV and 1 MeV and neutrons greater than 1 MeV within the pressure vessel. As neutrons propagate through the pressure vessel, the >1MeV flux decreases much more rapidly than the 100 keV - 1 MeV flux. Thus the flux ratio increases as neutrons propagate further from their source. This effect is even more dramatic in the upper portions of the pressure vessel.

Ex-Core Detector Response

One of the principal applications of this method is to compute ex-core detector response. The Model Problem 1 geometry has been used, with the following modifications: Model Problem 2 has added two ex-core power range detectors outside of the pressure vessel adjacent to the concrete wall, and Model Problem 2 has also reduced the spatial detail within the pressure vessel. The Model Problem 2 geometry is shown in Figures 7 and 8.

The core source regions are defined exactly the same as in Problem 1. The ex-core detectors have been sub-divided into 34 axial regions. This results in 17,340 (510x34) transport kernels for each detector. Again, a spatially flat source is defined within each source volume. The transport kernels are defined as the boron-10 absorption rate within each detector volume, for specified energy groups as well as integrated over all energies. Since this is a predominately thermal reaction, a different set of splitting/rouletting weights from Model Problem 1 has been used. The neutrons which ultimately interact within the detector are fast neutrons which leak out of the core and slow down in the vicinity of the detector. A total of 150 million histories were analyzed. This resulted in 2σ uncertainties of ~2-4% for each axial detector region.

Figures 9 and 10 show the relative contribution to detectors #1 and #2, respectively, from each core assembly. The kernels have been axially integrated, divided by the total detector response, and converted to percent. For example, Figure 9 shows that the two assemblies nearest detector #1 contribute 75% of the total detector response. Note that the percentages apply to this 1/8 core model only; a larger core model would show that the outermost assemblies azimuthally adjacent to the highest worth assemblies would also contribute significantly to detector response. However, Figures 9 and 10 show very clearly that the majority of detector response comes from the few assemblies nearest to each detector. If these assemblies were further sub-divided, the majority of the detector response would come from the outermost edges of these assemblies.

Figure 11 illustrates transport kernels vs. core height for the two highest worth assemblies with respect to detector #1. The data are presented in two ways: the detector kernels, i.e., weighted with a flat source distribution, and the detector kernels weighted with a representative core power distribution (for the purposes of illustration this is a simplified 3-D power distribution). This figure illustrates again how the transport kernels can be combined with any number of core source distributions. Finally, Figure 12 presents transport kernels vs. detector height from a single core source node. This figure illustrates that in addition to integrated or total detector response information, detailed detector response data may be obtained.

SUMMARY

This paper describes a powerful transport technique consisting of Monte Carlo generated transport kernels from a set of source regions to specific volumes of interest. The resulting transport kernels can be combined with any number of power distributions to determine response at various core conditions. The transport solution is exact, within the limits of physics and cross section approximations in RACER Monte Carlo code, except for statistical uncertainties. All kernels are generated simultaneously in one computer run, and no normalization or correction factors are involved.

REFERENCES

1. Brown, F.B., "Vectorization of 3-D General-Geometry Monte Carlo," *Trans. Am. Nuc. Soc.*, **53**, p. 283, 1986.

2. Gamino, R.G., Brown, F.B., and Mendelson, M.R., "A Monte Carlo Green's Function Method for Three-Dimensional Neutron Transport," *Trans. Am. Nuc. Soc.*, **65**, p. 237, 1992.

3. Bell, G.I. and Glasstone, S., *Nuclear Reactor Theory*, p. 20, Kreiger Publishing Company, Malabar, Florida (1968).

Figure 1 3-D Reactor Plant Model Problem 1 (Radial View)

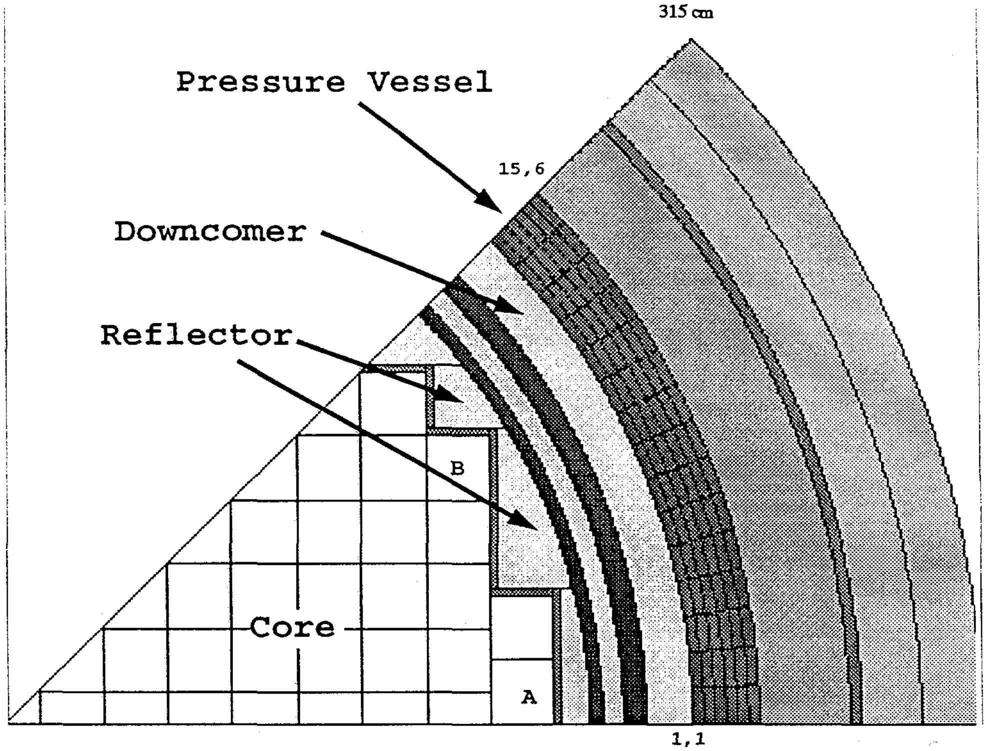

Figure 2 3-D Reactor Plant Model Problem 1 (Axial View)

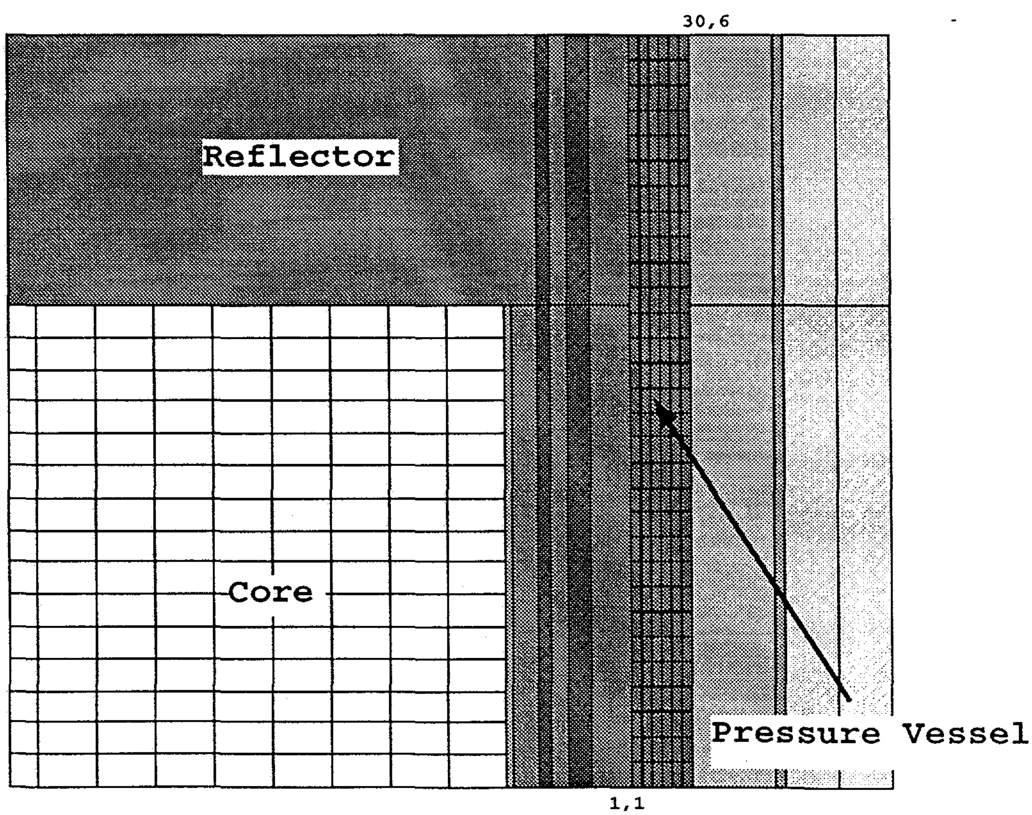

Figure 3 - Total Pressure Vessel Flux at First Axial Node > 1MeV Flux

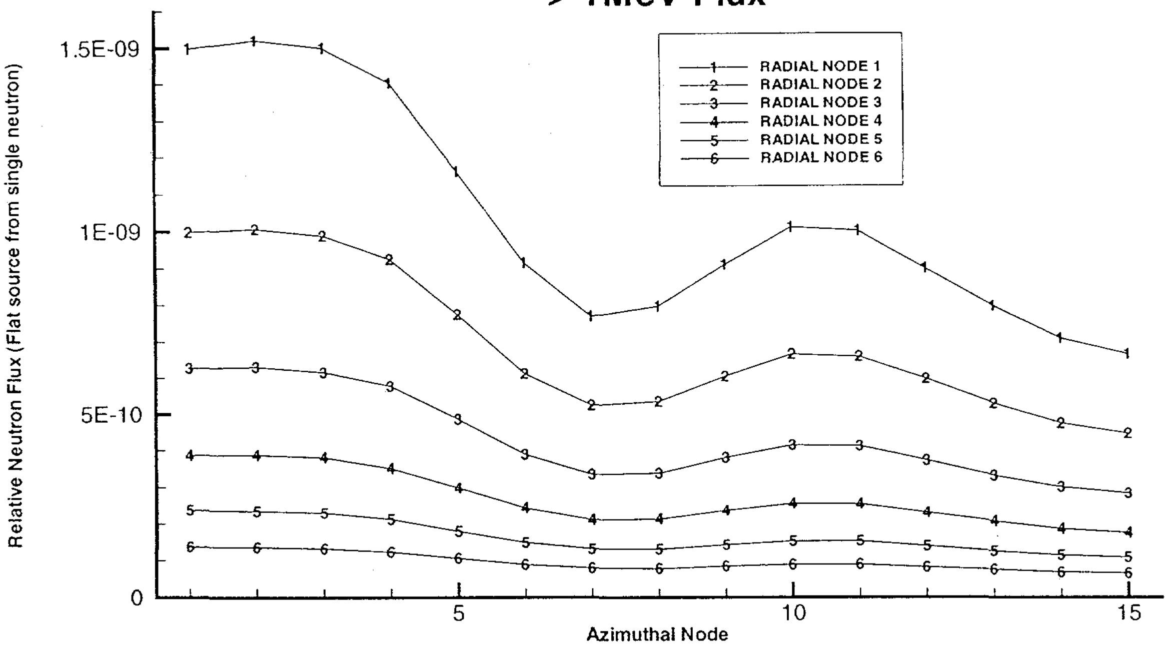

Figure 4 - Total Pressure Vessel Flux at First Azimuthal Node > 1MeV Flux

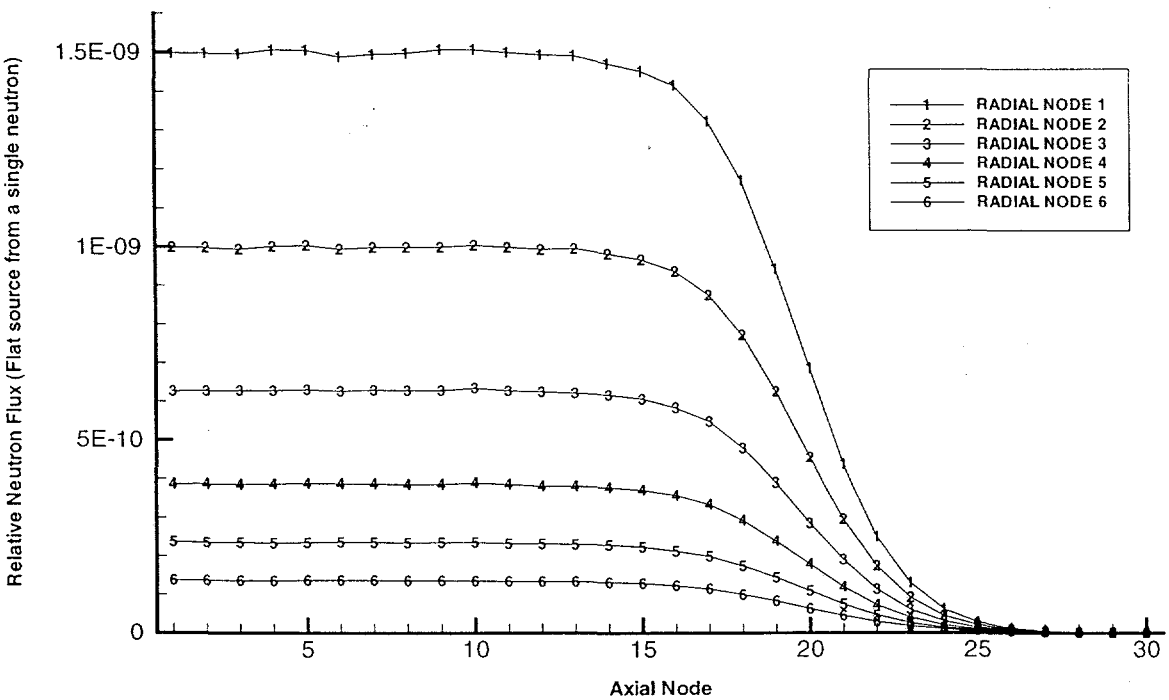

Figure 5 - Pressure Vessel Flux Response Kernels > 1MeV Flux

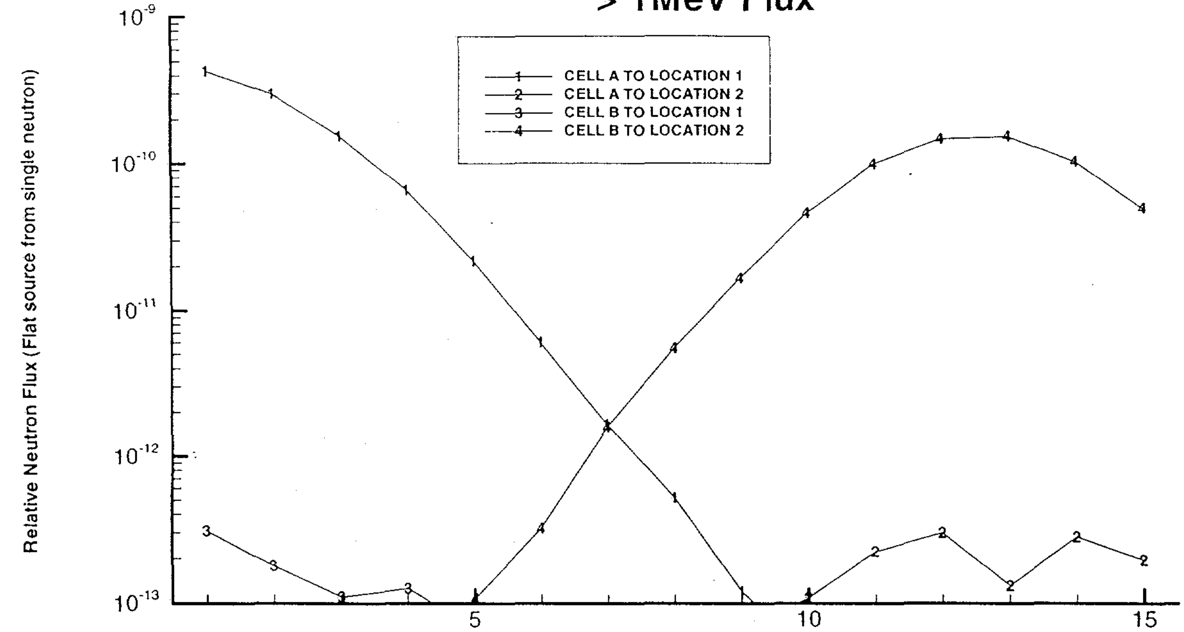

Location 1 - Pressure Vessel Axial,Radial, and Azimuthal Node 1

Location 2 - Pressure Vessel Azimuthal Node 10, Radial Node 1, Axial Node 15

Figure 6 - Ratio of Pressure Vessel Flux at First Azimuthal Node

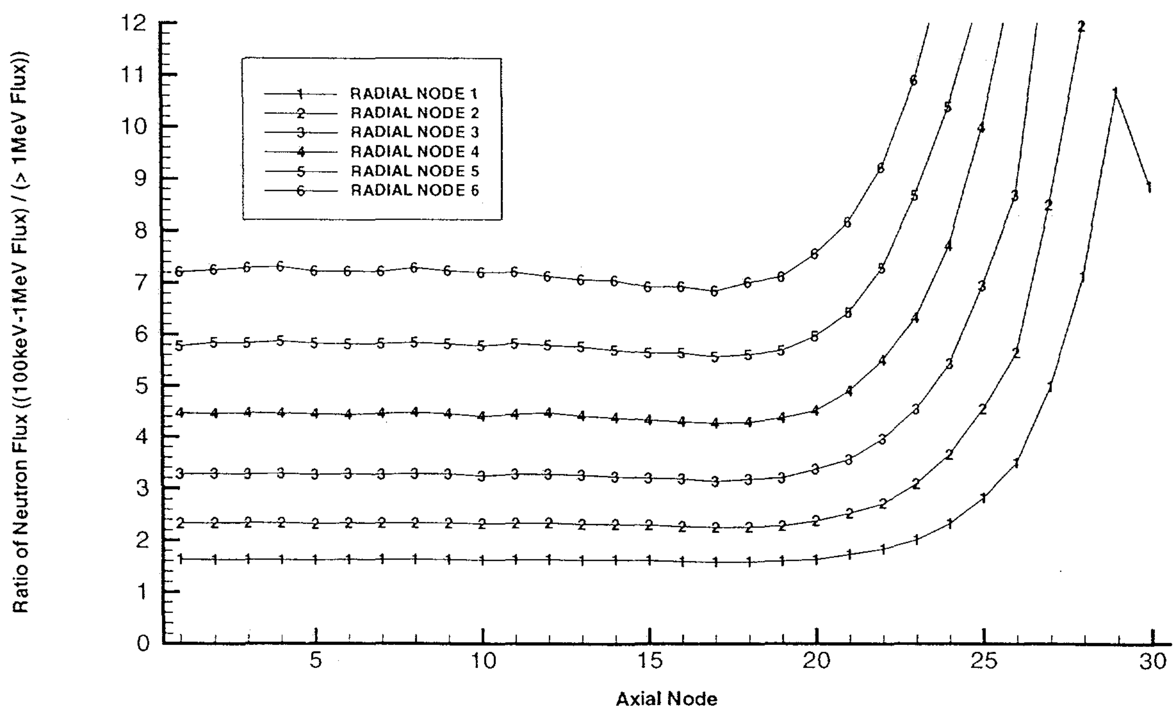

Figure 7. Horizontal Cross Sectional View of Problem 2

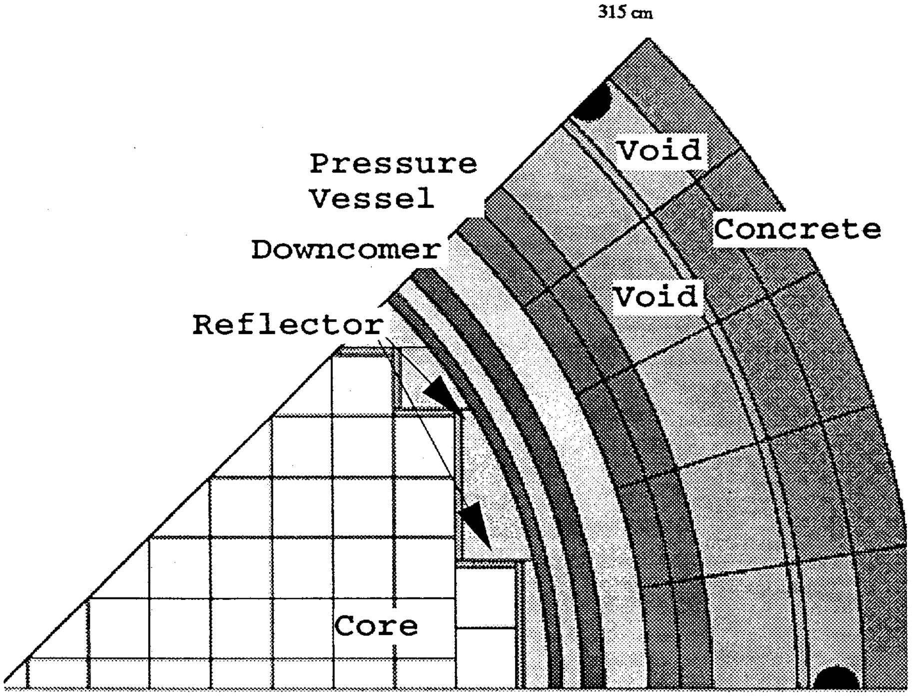

Figure 8. Vertical Cross Sectional View of Problem 2

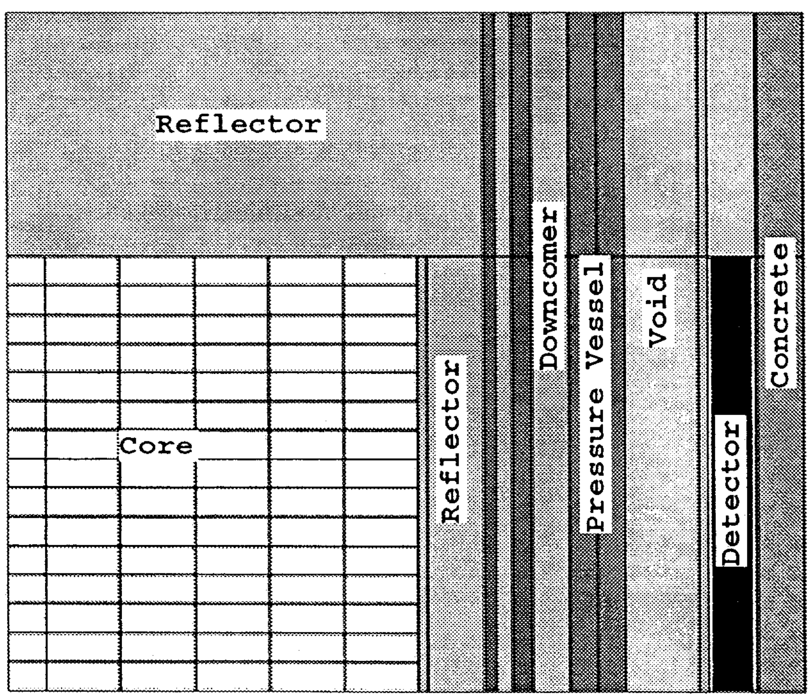

Figure 9. Axially Integrated Percent of Detector #1 Response from a Flat Source

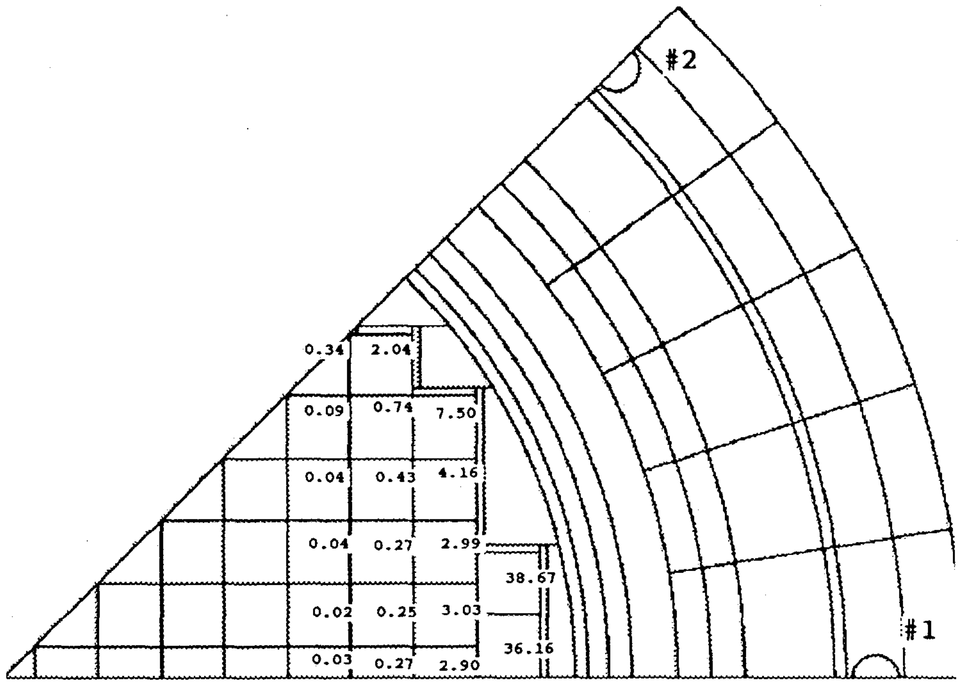

Figure 10. Axially Integrated Percent of Detector #2 Response from a Flat Source

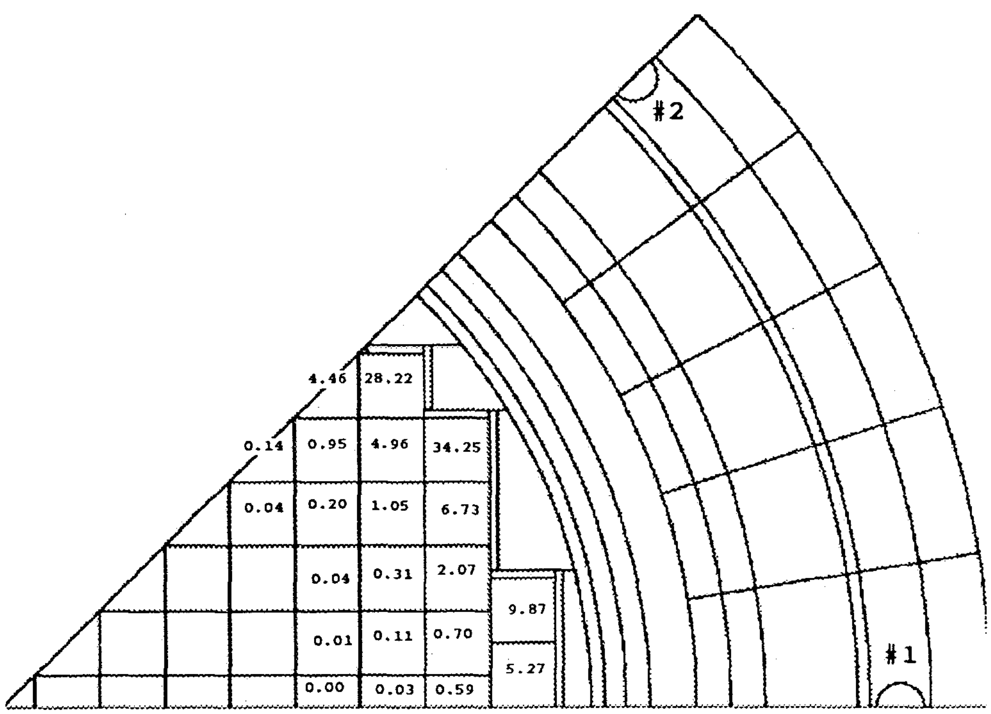

Figure 11. Total Detector Response from Two Assemblies
Transport Kernels vs. Core Height

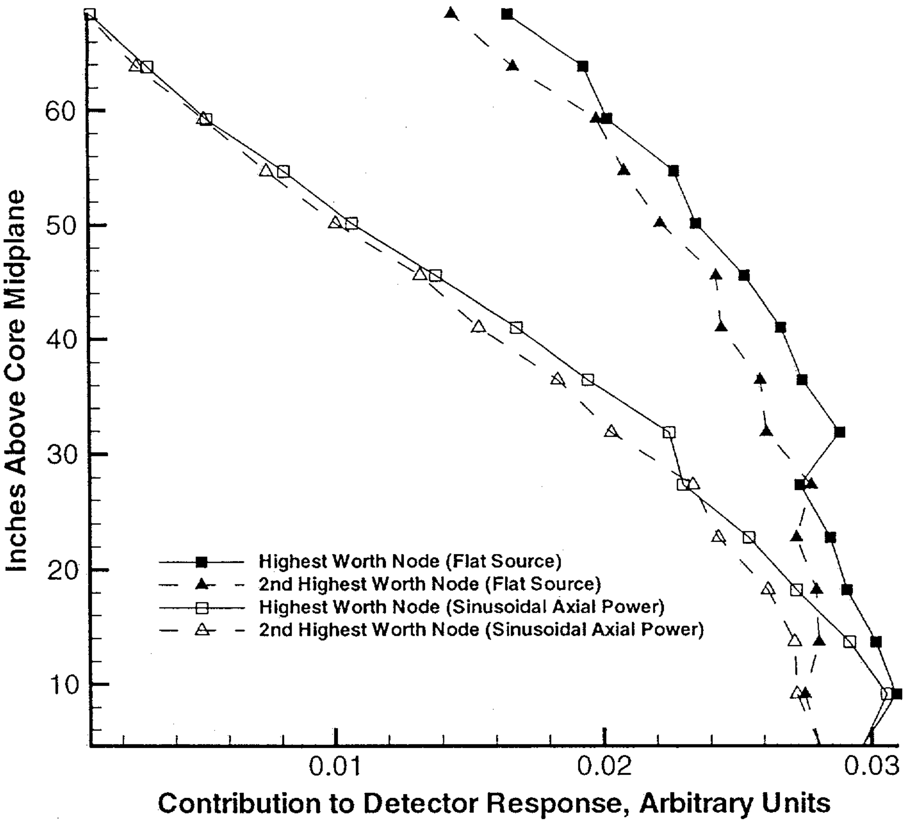

Figure 12. Detector Response from Single Source Node (31.9" - 36.5")
Transport Kernels vs. Detector Height (Detector #1)